

# An Apparatus for Production of Isotopically and Spin-Enriched Hydrogen for Induced Polarization Studies

Ayelet Gamliel · Hyla Allouche-Arnon ·  
Ruppen Nalbandian · Claudia M. Barzilay ·  
J. Moshe Gomori · Rachel Katz-Brull

Received: 10 June 2010/Revised: 29 July 2010/Published online: 16 September 2010  
© Springer-Verlag 2010

**Abstract** An apparatus for the production of hydrogen for hydrogenation-induced polarization studies was developed. The apparatus provides hydrogen gas from a solid source, thereby simplifying the requirement for siting of the apparatus. The produced hydrogen can be either isotopically enriched (with deuterium) or spin-enriched (with parahydrogen). These specialty gases were produced at small predetermined quantities and ambient pressure. The properties of the hydrogen mixtures were characterized by gas-phase nuclear magnetic resonance. The  $T_1$  of the

---

**Electronic supplementary material** The online version of this article (doi:[10.1007/s00723-010-0161-9](https://doi.org/10.1007/s00723-010-0161-9)) contains supplementary material, which is available to authorized users.

---

A. Gamliel · H. Allouche-Arnon · R. Nalbandian · J. M. Gomori · R. Katz-Brull (✉)  
Department of Radiology, Hadassah-Hebrew University Medical Center, Jerusalem, Israel  
e-mail: rkb@hadassah.org.il

A. Gamliel  
e-mail: gayelet@hadassah.org.il

H. Allouche-Arnon  
e-mail: ahyla@hadassah.org.il

R. Nalbandian  
e-mail: ruppen@hadassah.org.il

J. M. Gomori  
e-mail: gomori@hadassah.org.il

C. M. Barzilay  
Department of Medicinal Chemistry, School of Pharmacy,  
Hebrew University of Jerusalem, Jerusalem, Israel  
e-mail: claudiab@ekmd.huji.ac.il

*Present Address:*

C. M. Barzilay  
Bargal Analytical Instruments, Airport City, Israel

hydrogen mixtures (3.7 ms) was not affected by para-enrichment. The line width of the hydrogen signal in the para-enriched mixture was 34% larger. The reaction of ethyl propiolate hydrogenation served to evaluate the performance in terms of the ability to create hyperpolarized states. In this reaction, a polarization of 11.2% was measured for protons. Consecutive alkene hydrogenations as well as hydrogenations of the catalyst ligand resulted in additional hyperpolarized signals which were systematically assigned.

## 1 Introduction

The parahydrogen-induced polarization (PHIP) methodology has been studied since the mid-1980s [1–6] and gained renewed interest following the application of this concept for producing contrast in *in vivo* magnetic resonance imaging (MRI) [7–10]. Particularly attractive is the ability to transfer the increased spin order of the parahydrogen molecule to a neighboring nucleus such as carbon-13 or nitrogen-15 in a hydrogenated molecule and create, in effect, multinuclear “hyperpolarized” molecular probes. Upon administration of such hyperpolarized molecular probes to the circulation, “background free” images can be obtained using *in vivo* multinuclear imaging [7, 9]. A parallel approach for obtaining such background free images, and specifically spectroscopic images, is the dynamic nuclear polarization (DNP) approach [11–13]. The main advantage of this methodology is its ability to create the hyperpolarized state in many types of molecular sub-structures. However, the main disadvantage of this technology is the costly DNP apparatus and maintenance, combined with the long time (more than 30 min) of a single sample preparation. The main advantages of the PHIP methodology are its possible low-tech setup and the quick preparation of the hyperpolarized sample (few seconds). The latter offers a major advantage for dynamic biological studies and especially to *in vivo* studies.

The ability of the PHIP methodology to achieve enhancement of nuclear magnetic resonance (NMR) signals of two to four orders of magnitude for *in vitro* and *in vivo* applications has been well documented [7, 14–16]. The performance of the parallel approach, the orthodeuterium-induced polarization (ODIP), has been demonstrated only *in vitro* [4, 17]. Despite this wealth of information, the main challenge in implementing this technology is the practical setup of a PHIP or ODIP apparatus for cost-efficient and reproducible studies. Here, we report on such a PHIP apparatus that may serve for ODIP studies as well and characterize its performance.

Molecular hydrogen ( $H_2$ ) comprises two nuclear spin isomers, parahydrogen with opposed nuclear spins and orthohydrogen with parallel nuclear spins. At  $T > 298$  K, the equilibrium proportions are 25:75 para:ortho, respectively, and this mixture is referred to as “normal hydrogen” [18]. Below that temperature the equilibrium ratio increases, such that a 52:48 equilibrium ratio exists at liquid nitrogen temperature (77 K) [5].

On the other hand, in the deuterium molecule ( $D_2$ ), the orthodeuterium spin isomer is always dominant. The fraction of orthodeuterium is ca. 67% at room temperature and increases to 70% and ca. 98% at 77 and 20 K, respectively. In order

to reach a mixture that is significantly enriched with the orthodeuterium spin isomer and demonstrate the ODIP effect, a low temperature ( $T < 65$  K) [4, 17] is needed.

We have designed and implemented an apparatus for PHIP studies which may, pending further development, also serve for ODIP studies. Due to the relatively high temperature used here (77 K), the actual ODIP effect had not been demonstrated. However, generation of  $D_2$  gas is demonstrated and the means for its future spin enrichment are described.

The apparatus is composed of three main components: (1) a hydrogen source (for either  $H_2$  or  $D_2$ ); (2) a spin conversion system; and (3) a unit that regulates pressure. In addition, we describe a hydrogen injection system and a hydrogenation reactor containing solvent, hydrogenation catalyst, and reactants. The specific design described here takes into consideration the following desired features of such a system: (1) local production of hydrogen in sufficiently small amounts to avoid the risk of explosion; (2) minimization of heat exchange in the spin conversion system, to create two different temperature zones (room temperature and liquid nitrogen); (3) complete immersion of the spin conversion catalyst in the cooling liquid, to avoid back conversion at room temperature; and (4) immediate use of the spin converted hydrogen.

For production of hydrogen, we have relied on extensive knowledge that accumulated with regard to the “hydrogen economy”, an alternative suggested to substitute the non-sustainable fossil fuel-based economy. The reactions developed in this field provide the basis for supplying hydrogen to fuel cells [19]. Of the various approaches for in situ hydrogen generation described in the literature [19, 20], we have selected the sodium borohydride reaction with water specifically because it was commercially available both in the hydride and the deuteride form. In general, the supply of hydrogen in small quantities is safer; however, we note that sodium borohydride itself and its reaction with water are not completely harmless and the reaction should be carried out with the appropriate precautions. In the past, hydrogen for PHIP or ODIP studies was supplied by means of pure gas (pressurized tank) or by water hydrolysis.

The NMR properties of the hydrogen mixtures produced by this apparatus and thereby, the performance of this apparatus were characterized using the NMR-visible spin isomer of  $H_2$ , namely, orthohydrogen. Then, the ability to produce PHIP effects with the para-enriched mixtures was investigated in two in situ alkyne hydrogenations, which were previously shown useful in generating such effects. These reactions include the hydrogenation of ethyl propiolate [5] and ethyl phenylpropiolate [21]. We note that these reactions are not bio-compatible and were carried out at low yield.

## 2 The PHIP Apparatus: Description of Parts and Operation (With Notes Regarding ODIP)

The assembled apparatus is shown in Fig. 1. This apparatus contains three main parts: (1) a part that produces the hydrogen gas—the hydrogen production reactor

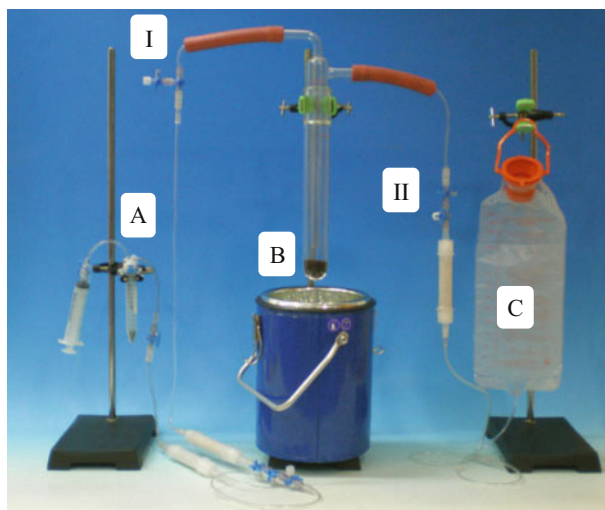
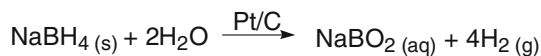


**Fig. 1** Apparatus for production of isotopically and spin-enriched hydrogen for induced polarization studies. *A* Hydrogen production unit, *B* spin conversion unit, *C* sealed plastic bag for regulating pressure

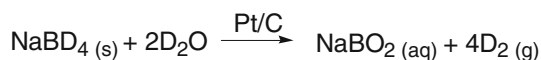
(Fig. 1A); (2) a spin conversion part which facilitates the spin conversion of the hydrogen molecule ( $H_2$  or  $D_2$ ) with respect to the thermal equilibrium (Fig. 1B); and (3) a unit that regulates pressure (Fig. 1C).

## 2.1 Production of Hydrogen

Hydrogen ( $H_2$ ) or deuterium ( $D_2$ ) is produced by a chemical reaction of sodium borohydride or sodium borodeuteride with water or deuterated water ( $D_2O$ ), respectively, in the presence of platinum on carbon catalyst, as described in Schemes 1 and 2, respectively. These reactions take place in the hydrogen production reactor (Fig. 1A). Sodium borohydride and sodium borodeuteride are both solid compounds which allow for safe storage. Both are available in a powder form that allow quick production of small predetermined amounts of hydrogen ( $H_2$ ) and deuterium ( $D_2$ ). The hydrogen production reaction is started under vacuum. This is important in several aspects: (1) to ensure that gas accumulating in the



**Scheme 1** Production of hydrogen ( $H_2$ ) from sodium borohydride and water



**Scheme 2** Production of deuterium ( $D_2$ ) from sodium borodeuteride and deuterated water

system is exclusively hydrogen and therefore to perform subsequent hydrogenation reactions efficiently in terms of the purity level of hydrogen used; (2) to avoid the presence of oxygen in the system in order to avoid the risk of explosion/flammability of the hydrogen production reactor; and (3) to diminish the possibility of reducing the level of spin enrichment by interaction with oxygen or another air component.

## 2.2 Hydrogen Collection at Regulated Pressure

Hydrogen gas that is produced by this reaction flows through drying tubes (see Sect. 3.1) into the spin conversion part (Fig. 1B), which is inactive at room temperature, and is collected in a flexible sealed plastic bag (the collection bag). This bag serves as a unit that maintains production at ambient pressure (Fig. 1C). When sufficient amount of hydrogen has accumulated in the collection bag, extra hydrogen that might continue to be produced in the reactor is routed to another collection bag through outlet I (Fig. 1).

## 2.3 Spin Conversion Finger

The spin conversion occurs in a glass trap (Fig. 1B). The dimensions of this glass trap are as follows: height of 220 mm and diameter of 42 mm for the external cylinder; length of 170 mm and diameter of 10 mm for inner tube. The glass trap contains iron(III) oxide at its bottom (about 25 g). Iron(III) oxide was previously shown to catalyze the spin conversion at liquid nitrogen temperature [22]. Prior to the spin conversion, the reactor is sealed away from the spin conversion finger by the valve at position I (Fig. 1). Then the spin conversion finger is immersed in liquid nitrogen. This is done by lowering the glass trap into the Dewar (shown in Fig. 1) down to a level where the catalyst is about 10 cm below the liquid nitrogen level. This immersion in liquid nitrogen results in a quick decrease in the gas volume. This is visible as a substantial decrease in the volume of the plastic bag. Hydrogen gas accumulates at the bottom of the cold finger next to the iron oxide catalyst. To isolate hydrogen undergoing spin conversion from hydrogen that may remain in the collection bag, the passage between the two compartments is blocked by the valve at position II (Fig. 1).

This setup was designed in order to enable free passage of hydrogen between two temperature zones: a liquid nitrogen temperature (where the catalyst is placed and hydrogen undergoes spin conversion) and room temperature (where gas is found in a state amenable for withdrawal from the apparatus). Hydrogen that underwent spin conversion in the cold zone does not undergo back spin conversion at room temperature because the catalyst is located exclusively in the cold zone and the transition without a catalyst is a forbidden one.

Many of the systems that are described in the literature use a metal tube for the spin conversion part [4–6, 23]. The choice of a glass trap was made due to two reasons: first, because the glass is transparent, the exact location of the catalyst is readily known. This is important because iron oxide (or other spin conversion catalyst) catalyzes the conversion not only from ortho to para but also from para to

ortho (at room temperature). If there is any catalyst at room temperature, some of the para-enriched mixture may convert back to the ortho state and the overall efficiency of the system may decrease. The second reason for using the glass trap is the low thermal conductivity of the glass. It is expected that the heat exchange from the surrounding to liquid nitrogen through the glass is much lower than the heat exchange that occurs when copper tubes or other kind of metal tubes are used [23]. Indeed, the upper part of the trap was at room temperature while the lower part of the trap was placed in liquid nitrogen.

## 2.4 Utilization of Enriched Hydrogen

Enriched hydrogen is taken out of the spin conversion finger via outlet II (Fig. 1) and used immediately. The spin ratio of ortho to para hydrogen is expected to increase with time at liquid nitrogen temperature. However, the specific ratio at a specific time duration would be related to the catalyst surface area available to the hydrogen molecules and the total amount of hydrogen undergoing conversion. Here, the level of spin conversion was quantified at ca. 2 and 4 h in liquid nitrogen and reached approximately 46% parahydrogen at 4 h (as described in Sect. 4). However, significant PHIP effects were obtained already after 1 h in liquid nitrogen (see Sect. 4). We note that the apparatus described here produced about 600 ml of spin-enriched H<sub>2</sub> per batch, which is sufficient for about 120 PHIP reactions (under conditions described herein).

## 3 Experimental

### 3.1 Materials

Sodium borohydride, sodium borodeuteride, 1 wt% platinum on activated carbon (1% Pt/C), ethyl propiolate, ethyl phenylpropiolate, acetone-d<sub>6</sub>, and (1,5-cyclooctadiene)1,4-bis(diphenylphosphino)butane rhodium (I) tetrafluoroborate [Rh(COD)(dppb)BF<sub>4</sub>] were purchased from Sigma-Aldrich (Rehovot, Israel). Plastic drying tubes for gases were purchased from Sigma-Aldrich and were filled with Molecular Sieve Dehydrate Fluka with indicator for drying gases (Sigma-Aldrich).

### 3.2 NMR

NMR measurements were carried out at 11.8 T (Varian Inc., Palo Alto, CA). Proton spectra were acquired with either direct or indirect detection 5 mm probes. <sup>2</sup>H and <sup>13</sup>C spectra were acquired with a broadband direct detection probe.

### 3.3 Hydrogen and Deuterium Production

Sodium borohydride or sodium borodeuteride (0.7 g) and 1% Pt/C (150 mg) were placed in a 15 ml plastic tube and combined with 3 ml of purified water under

vacuum (see Sect. 2). Under these conditions, about 600 ml of hydrogen or deuterium was produced within 20 min.

### 3.4 Gas-Phase Studies

Prior to the gas-phase NMR measurements, NMR tubes (5 mm, Wilmad, NJ, USA) were thoroughly washed with 3% HCl, then washed with purified water containing 30 mM ethylenediaminetetraacetic acid, and then dried. Hydrogen was injected in excess into the NMR tube in an inverted position at ambient pressure using a long NMR pipette (Wilmad, NJ, USA). The tube was then sealed with polytetrafluoroethylene NMR tube caps (Sigma-Aldrich, Rehovot, Israel), and immediately transferred in an inverted position to the NMR spectrometer. Above the spectrometer bore, the tube was turned to an upright position and immediately measured.

### 3.5 H<sub>2</sub> Spin Enrichment

<sup>1</sup>H NMR spectra were recorded using 320 averages, 55 ms relaxation delay, and a 90° flip angle. The enrichment of the hydrogen mixture with the para spin isomer was determined by comparing the intensities of the NMR-visible orthohydrogen signal (signal height multiplied by the full width at half-height). Normal hydrogen (see above) and enriched mixtures were sampled prior to and during the time that the spin conversion finger was immersed in liquid nitrogen, respectively. The data were analyzed using Matlab (The Mathworks Inc., Natick, MA).

### 3.6 T<sub>1</sub> and T<sub>2</sub> Measurements of H<sub>2</sub> Mixtures

T<sub>1</sub> measurements of H<sub>2</sub> mixtures were performed with the standard inversion–recovery pulse sequence using 320 averages per inversion delay and a relaxation delay of 55 ms. T<sub>2</sub> measurements of H<sub>2</sub> mixtures were performed with the Carr–Purcell–Meiboom–Gill (CPMG) pulse sequence. Calculation of T<sub>1</sub> and T<sub>2</sub> was performed using the curve-fitting tool in Matlab (The Mathworks Inc., Natick, MA).

### 3.7 Isotopic Enrichment, <sup>2</sup>H-NMR

D<sub>2</sub> spectra were acquired using 1,024 averages, 90° flip angle, and 60 ms relaxation delay.

### 3.8 PHIP Studies

Hydrogen was injected into a 5 mm NMR tube containing the reaction mixture, via PEEK tubes (outer diameter, 1.6 mm, inner diameter, 1 mm, Upchurch Scientific, Washington, USA) through rubber septa (Wilmad, NJ, USA). The rate of the injection was 5 ml per 5 s. A small (ca. 1 mm) opening at the top of the NMR tube allowed gas outflow and ambient pressure conditions. For ALTADENA (adiabatic longitudinal transport after dissociation engenders nuclear alignment) experiments [24], the reaction was carried out inside a magnetic shield (two concentric tubes, 10

and 15 cm in diameter, 50 cm long, Mu-Metal, The MuShield Company, New Hampshire, USA) and the hyperpolarized  $^1\text{H}$  spectrum was recorded about 15 s after the injection (one transient at minimal receiver gain). The magnetic field inside the shield was of the order of a few nT, as per manufacturer specifications. Performing the hydrogenation reaction inside the shield ensured zero interference of the spectrometer's fringe field that could lead to mixed ALTADENA and PASADENA (parahydrogen and synthesis allow dramatically enhanced nuclear alignment) effects. For PASADENA experiments [5], the same reaction using the same hydrogen injection system and conditions was performed inside the spectrometer, and the spectrum was recorded immediately after the end of the hydrogen injection (one transient, minimal gain). Both PASADENA and ALTADENA PHIP studies were carried out using  $45^\circ$  pulses as previously described [5].

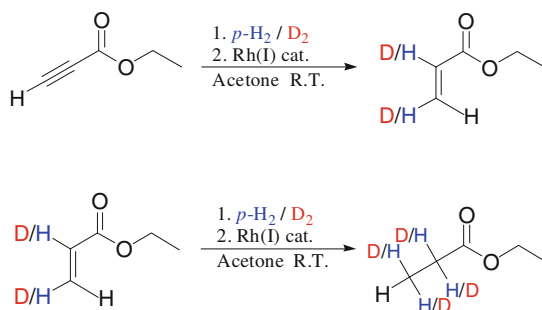
The enhancement factor was calculated by comparing the integration of the PHIP signal to that of the product signal after relaxation (via intensity comparison of both signals to the substrate signal). Both signals were compared on the basis of their intensity in a single scan following a single hydrogenation (injection of 5 ml  $\text{H}_2$  at ambient pressure). The concentration of each was deduced by comparison to the substrate signal, accounting for the reaction yield. However, because the thermal equilibrium signal of the ethyl acrylate that was produced following a single hydrogenation was small and close to the detection threshold, the intensity of this signal was calculated using a spectrum showing the product of 10 hydrogenations with 128 transients and optimal gain.

For  $^{13}\text{C}$  hyperpolarization studies, the enhanced spin order of the  $\text{H}_2$  molecule was transferred to  $^{13}\text{C}$  at natural abundance by means of magnetic field changes, similar to previously described magnetic field cycling [7, 10, 25, 26]. In fact, the hydrogenation reaction and timing for both proton and carbon-13 ALTADENA studies was the same. Specifically, the hydrogenation reaction was performed at low magnetic field (of the order of nT) which was achieved using the Mu-Metal shield. Within 15 s, the sample was taken out of the magnetic shield, moved through the fringe field of the magnet, and placed in the spectrometer. A single  $^{13}\text{C}$  spectrum was recorded immediately. The full intensity solvent signals were used as an internal standard for concentration and enhancement factor calculation. These were acquired after the hyperpolarization decay using a long relaxation delay ( $>20$  s) prior to the acquisition.

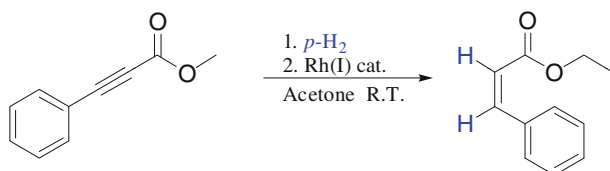
## 3.9 Reaction Conditions

### 3.9.1 Ethyl Propiolate Hydrogenation (Scheme 3)

The reaction mixture contained ethyl propiolate (214 mM in 700  $\mu\text{l}$  acetone- $d_6$ ) and the rhodium catalyst  $[\text{Rh}(\text{I})(\text{COD})(\text{dppb})]\text{BF}_4$  (10 mg, 20 mM). Similar conditions were described by Jonischkeit et al. [5]. High-intensity PHIP signals are observed when  $\text{H}_2$  enriched in the para spin state is added in a pair-wise manner to a metal center or an unsaturated substrate while spin correlation between the two protons is maintained [22]. This specific rhodium catalyst was chosen as a simple but efficient, commercially available catalyst precursor that had already shown ability to produce large PHIP signals [5].



**Scheme 3** In situ hydrogenation of ethyl propiolate to ethyl acrylate and subsequent hydrogenation to ethyl propionate



**Scheme 4** In situ hydrogenation of ethyl phenylpropiolate to ethyl cinnamate

### 3.9.2 Ethyl Phenylpropiolate Hydrogenation (Scheme 4)

The reaction mixture contained ethyl phenylpropiolate (216 mM in 700  $\mu\text{l}$  acetone- $\text{d}_6$ ) and the rhodium catalyst  $[\text{Rh}(\text{I})(\text{COD})(\text{dppb})]\text{BF}_4$  (13 mg, 25 mM). Similar conditions were described by Jonischkeit et al. [21].

## 4 Results and Discussion

An apparatus for production of spin- or isotopically enriched hydrogen for hyperpolarization studies is described above and is shown in Fig. 1. This apparatus was used to generate hydrogen mixtures that are either spin-isomer enriched (the para spin isomer for  $\text{H}_2$ ) or isotopically enriched ( $\text{D}_2$ ).

### 4.1 Parahydrogen Enrichment

The effect of hydrogen mixture enrichment with the para spin isomer can be seen in Fig. 2. Since only the ortho spin isomer is NMR visible, the signal of the para-enriched mixture is of lower area (ca. 1.33:1 area ratio of non-enriched:enriched). This area ratio was converted to % enrichment taking into account the natural distribution at room temperature, in which 25% of hydrogen in the mixture consists of the para spin isomer. The level of para-enrichment reached  $42.3 \pm 0.4\%$  ( $n = 4$ ) following  $127 \pm 9$  min in liquid nitrogen. This level had increased with the time of spin conversion (in liquid nitrogen), reaching  $46.3 \pm 1.3\%$  ( $n = 4$ ,  $P = 0.0045$ , paired, two-tail,  $t$  test) at  $221 \pm 11$  min. These values include data collected on three

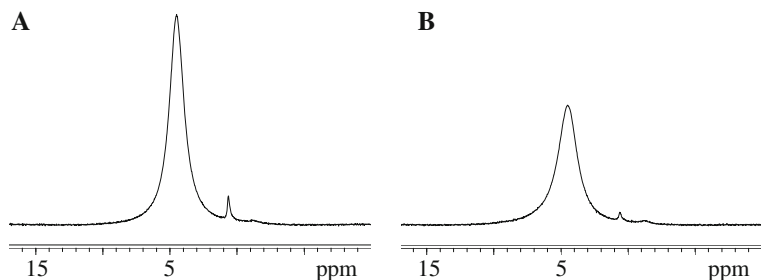


**Fig. 2** Typical orthohydrogen signal in “normal hydrogen” (a) and para-enriched hydrogen mixture (b)

different experimental days. We note that this increase was not linear with time in liquid nitrogen. The theoretical occupancy of the para spin isomer at liquid nitrogen temperature is 52%; therefore, the expected orthohydrogen signal ratio at room temperature equilibrium and at 77 K equilibrium is 1.56:1. We predict that given a longer immersion periods in liquid nitrogen, this equilibrium value can be attained.

#### 4.2 Hydrogen Mixtures Relaxation Times

Interestingly, the line width of the orthohydrogen signal in the para-enriched mixtures was wider than that of the “normal hydrogen” ( $840 \pm 44$  Hz,  $n = 15$ , and  $629 \pm 14$  Hz,  $n = 9$ , respectively,  $P = 2 \times 10^{-12}$ , two-tail,  $t$  test). For this reason, the  $T_2$  of the hydrogen mixtures was investigated. A typical CPMG experiment is shown in the Supplementary material. Indeed, the  $T_2$  of the para-enriched mixture was found to be shorter than that of the “normal hydrogen” ( $0.47 \pm 0.03$  ms,  $n = 3$ , and  $0.54 \pm 0.01$  ms,  $n = 3$ , respectively,  $P = 0.015$ , two-tail,  $t$  test). However, this decrease did not fully explain the increase in the line width of the signal. Also, we note that determination of the difference in such short  $T_2$ s may be close to the border of accuracy of the spectrometer as the difference is on the order of tens of  $\mu$ s which is close to the  $180^\circ$  pulse (ca.  $10 \mu$ s).

The  $T_1$  of the hydrogen mixtures was investigated as well. It was found that this relaxation time was not affected by the enrichment with the para spin isomer. A typical inversion–recovery experiment is shown in the Supplementary material. The  $T_1$  measured here for hydrogen mixtures at room temperature and ambient pressure was  $3.7 \pm 0.9$  ms,  $n = 14$ . To the best of our knowledge, the  $T_1$  of orthohydrogen in the gas phase was previously determined only in one publication [27]. In that study, low temperatures (34–40 K) were used at up to 40 atm, and very dilute orthohydrogen conditions, i.e., high levels of parahydrogen enrichment of 86–99.4%. The  $T_1$  of orthohydrogen under these conditions ranged from 2.7 to 14.5 ms.

#### 4.3 Hydrogen Gas Sample Stability

All of the above studies in the gas phase were carried out immediately upon withdrawal of the gas sample from the apparatus. However, to test the stability of

these samples in the NMR tube, fully relaxed spectra of the hydrogen mixtures were recorded for up to 20 min from the time of withdrawal. The level of orthohydrogen was found to be constant during this period. Therefore, it is not likely that any of the above measurements are affected by sample instability over the time frame of the measurement.

#### 4.4 D<sub>2</sub> Production

By exchanging sodium borohydride and H<sub>2</sub>O for sodium borodeuteride and D<sub>2</sub>O, the same apparatus was used for production of deuterium (D<sub>2</sub>). This reaction is shown in Scheme 2. As opposed to the H<sub>2</sub> mixture, where at liquid nitrogen the mixture reaches a significant excess of parahydrogen over “normal hydrogen”, the D<sub>2</sub> mixture is expected to reach only a small excess of orthodeuterium under the same conditions (70 vs. 67% at 77 K and room temperature, respectively) [28]. Therefore, as expected, the difference in the D<sub>2</sub> signal area in the mixtures that underwent spin conversion in liquid nitrogen and the mixtures at room temperature equilibrium was too low to be significantly measured. The signal area of the respective D<sub>2</sub> mixtures was  $2,127 \pm 97$ ,  $n = 3$  and  $2,167 \pm 110$ ,  $n = 3$  (normalized arbitrary units). Thus, the error in these measurements was larger than the expected difference in percent enrichment. Therefore, the change in signal intensity could not be determined.

#### 4.5 PHIP Performance

The ability to use para-enriched hydrogen produced by the apparatus in PHIP reactions was investigated using the alkyne in situ hydrogenation reactions described above. Specifically, the ethyl propiolate reaction was repeated numerous times to quantify and determine the reproducibility of the ALTADENA and PASADENA effects.

#### 4.6 Hydrogenation of Ethyl Propiolate

The in situ hydrogenation of ethyl propiolate to ethyl acrylate with the aid of a rhodium catalyst is described in Scheme 3. The ALTADENA and PASADENA PHIP spectra of this reaction are shown in Fig. 3. The averaged ethyl acrylate concentration per injection of 5 ml p-H<sub>2</sub> (para-enriched hydrogen) was 1.75 mM and the reaction yield was about 1% (Table 1). The <sup>1</sup>H-ALTADENA spectrum (Fig. 3a) demonstrates large signals of the hyperpolarized product at 5.85 and 6.15 ppm. The third vinylic hydrogen at 6.3 ppm is also enhanced, as previously described [29]. The spectrum in Fig. 3c was recorded after the decay of the hyperpolarized signal. The product signal at thermal equilibrium level is visible. The intensities of both the ALTADENA and PASADENA (Fig. 3b) hyperpolarized signals were expressed in concentration values, from which the average values of the enhancement factors were calculated (ca. 3,000 and 1,000, respectively, Table 1).

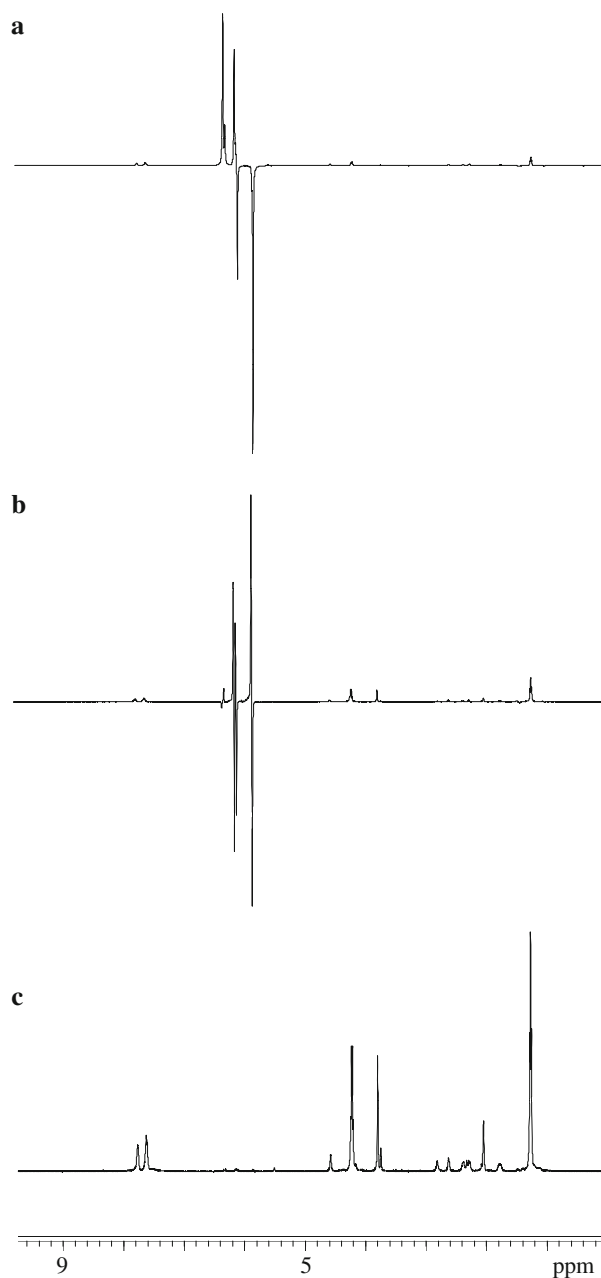


**Fig. 3** Phip  $^1\text{H}$  spectra of ethyl propiolate hydrogenation reaction. **a** ALTADENA spectrum, single transient recorded ca. 15 s after the para-enriched hydrogen injection (minimal gain). **b** PASADENA spectrum, single transient recorded immediately at the end of the enriched hydrogen injection (minimal gain). **c** Reference spectrum recorded after decay of the hyperpolarized signal in **a**. This spectrum is 22-fold enlarged in comparison to spectrum **a**, as evident from comparison of the intensity of the substrate signal at ca. 1.25 ppm in both spectra

**Table 1** PHIP reactions and effects observed in  $^1\text{H}$  spectra

Substrate/solvent	Ethyl propiolate/acetone	Ethyl phenylpropiolate/acetone
Reaction yield (%)	0.82 ( $n = 10$ )	0.23
Product concentration <sup>a</sup> (mM)	$1.75 \pm 0.4$ ( $n = 10$ )	$0.49$ ( $n = 4$ )
ALTADENA PHIP level (mM)	$5,578 \pm 2,824$ ( $n = 11$ )	$1,288^b$
ALTADENA enhancement factor	$3,187 \pm 1,614$ ( $n = 11$ )	$2,653^b$
PASADENA PHIP level (mM)	$1,975 \pm 314$ ( $n = 10$ )	$462^b$
PASADENA enhancement factor	$1,129 \pm 180$ ( $n = 10$ )	$953^b$

<sup>a</sup> Per one hydrogenation step, i.e., injection of 5 ml of para-enriched hydrogen mixture at ambient pressure

<sup>b</sup> Best result out of two studies

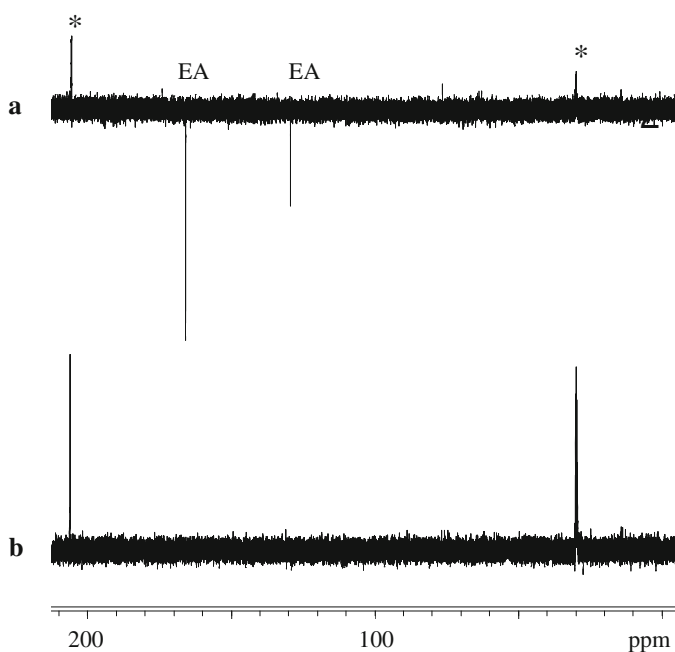


**Fig. 4** PHIP  $^{13}\text{C}$  spectra of ethyl propiolate hydrogenation reaction. **a**  $^{13}\text{C}$ -ALTADENA spectrum with field cycling. A single transient was recorded at high gain. **b**  $^{13}\text{C}$  spectrum of the same sample as in **a** after the decay of the hyperpolarized signal recorded with the same acquisition protocol and parameters. In addition, a relaxation delay of about 1 min was provided to allow the signals of the solvent to reach maximum intensity. Asterisk acetone signals, EA hyperpolarized ethyl acrylate signals

The results of a typical  $^{13}\text{C}$ -ALTADENA study are illustrated in Fig. 4. Figure 4a demonstrates the hyperpolarized product signals which were recorded using one transient. The spectrum in Fig. 4b was recorded after the hyperpolarization decay and after full alignment of the solvent signals with the main magnetic field (full intensity solvent signals). The averaged intensity of the hyperpolarized

signal at 167 ppm was equivalent to  $7,162 \pm 1,545$  mM ( $n = 4$ ) and the enhancement factor was calculated to be  $4,094 \pm 885$  ( $n = 4$ ).

#### 4.7 Hydrogenation of Ethyl Phenylpropiolate

The in situ hydrogenation of ethyl phenylpropiolate to ethyl cinnamate with the aid of a rhodium catalyst is described in Scheme 4. The ALTADENA and PASADENA PHIP spectra of this reaction are shown in the Supplementary material. The averaged product concentration and the reaction yield are summarized in Table 1. The maximal enhancement factors measured in these studies were ca. 2,700 and 1,000, respectively (Table 1).

#### 4.8 Enhancement Factor and Polarization Level Considerations

Previous studies reported on various orders of enhancement factors or polarization levels under varying experimental conditions. It is important to note that the enhancement factor and, therefore, the calculated polarization level depend critically on the combination of all of the experimental parameters such as the magnetic field strength and the temperature, at which data were recorded, the duration from reaction to recording, the level of parahydrogen enrichment, and the PHIP type of experiment (ALTADENA or PASADENA). Also, it is important to note whether the reported polarization levels are the measured ones or values obtained by extrapolation of the measured values taking into account the particular  $T_1$  and the duration to recording. For this reason, comparing the performance of our apparatus to previously published studies is not straightforward. Nevertheless, a short review of several relevant publications is given as follows.

For protons, after enrichment at 77 K, in an ALTADENA type of study: a polarization level of 0.3% (corresponding to ca. 670 enhancement factor) had been obtained at 1.5 T [7]; an enhancement factor of 300 was obtained in the gas phase at 7 T (corresponding to 0.6% polarization) [15]; and an enhancement factor of 12,000 (corresponding to 17.7% polarization) was obtained at 4.7 T [5]. At the same conditions, an enhancement factor of 1,800 was obtained in a PASADENA type of study [5].

For carbon-13, using the PASADENA approach, a signal enhancement of 4,400 [9] (corresponding to 0.49% polarization) and a polarization level of  $-4\%$  [7] had been reported at 1.5 T, and an enhancement factor of 37,400 corresponding to ca. 13% polarization was obtained at 4.7 T [16]. The latter represents an estimate of the initial polarization based on the measured enhancement factor, the duration to recording, and the product  $T_1$ . Using a hydrogen mixture that was about 98% enriched with parahydrogen (at 14 K), the  $^{13}\text{C}$  signal enhancement at 7 T in an ALTADENA type of study was found to be  $-37,700$ , corresponding to a polarization of  $-21\%$  [10].

Here, using enrichment at 77 K, we report on an averaged 3,187 enhancement factor for protons in an ALTADENA study (Table 1) at 11.8 T, corresponding to 11.2% polarization. For  $^{13}\text{C}$ , we report on 3.8% polarization at the time of the

recording. The PHIP effects and the corresponding polarization levels obtained with the current apparatus (Table 1) are within the range described previously.

We note that current studies were performed at 11.8 T where the polarization at thermal equilibrium is higher (linearly with the field) and therefore the expected enhancement factor is proportionally lower. The enhancement is commonly evaluated with respect to the thermal equilibrium state. However, the signal intensity obtainable from the thermal equilibrium state depends on the magnetic field strength ( $B_0$ ) and the temperature ( $T$ ) and is proportional to  $\gamma B/kT$ , where  $\gamma$  is the gyromagnetic ratio and  $k$  is the Boltzmann constant. Therefore, even though the  $p\text{-H}_2$ -derived polarization is field-independent, the enhancement factor does depend on the magnetic field in which the thermal equilibrium state is established [5, 15].

In addition, we note that several previous studies consider the extrapolated enhancement factor, taking into account the duration between the PHIP generation and the actual measurement. However, the data presented here correspond to actual and not to extrapolated enhancement factors. The actual enhancement factors provide relevant order-of-magnitude data for future biomedical applications.

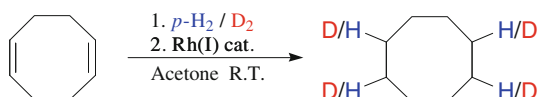
#### 4.9 The PHIP Signals

The data summarized in Table 1 emphasize the various parameters that affect the PHIP signals. For example, the reaction yields: the reaction yield and the product concentration are about four folds higher in the reaction of ethyl propiolate, compared to ethyl phenylpropiolate. In agreement, the signal intensity for the latter reaction is fourfold lower for both ALTADENA and PASADENA experiments. However, we note that the reaction yield and the product concentration per se cannot serve as sole predictive factors to the PHIP effect which is reaction dependent.

#### 4.10 PHIP Signals from Other Products

Interestingly, in the two reactions described here and in most other alkyne reactions carried out at our laboratory, in addition to the expected vinyl PHIP signals, a PHIP signal has been continuously observed also at ca. 1.5 ppm. To reveal the source of this signal, a series of studies was carried out using the reaction of ethyl propiolate hydrogenation (Scheme 3). This series is described in the Supplementary material. The source of the PHIP signal at 1.5 ppm was identified as cyclooctane which resulted from hydrogenation of cyclooctadiene—one of the catalyst ligands (Scheme 5). Additional signals at ca. 2.25 ppm and at 1.05 ppm were attributed to ethyl propionate, the product of the sequential hydrogenation of ethyl acrylate (Scheme 3), and the signal at ca. 5.6 ppm was attributed to cyclooctene, the product

**Scheme 5** Hydrogenation of the COD ligand to cyclooctane



of a single hydrogenation of the COD ligand [14]. Explanatory notes for these assignments are provided as Supplementary material.

## 5 Conclusion

The apparatus described herein is compact, cost-efficient, and aids in the generation of small predetermined amounts of hydrogen (either H<sub>2</sub> or D<sub>2</sub>). The parahydrogen enrichment level reached by the apparatus and the consecutive polarization levels reached in the ALTADENA studies on the ethyl propiolate reaction are within the range of previously published reports. The system proved to be an adequate source of parahydrogen for PHIP studies in a biomedical environment.

**Acknowledgments** We thank Aaron K. Grant, Elena Vinogradova, and Robert E. Lenkinski for useful discussions during the course of this work. We thank Magnus Karlsson for helpful discussions on gas-phase NMR measurements. We thank Shimon Vega for discussions on orthodeuterium. This study has been supported in part by the DANA foundation, the Bi-National Science Foundation (BSF, grant number 2006118), the German Israel Foundation (GIF, grant number 2131-1586.5/2006), the Abisch-Frenkel Foundation, and the Center for Complexity Science (grant number GR2007-053). R.K.B thanks the generosity of the Tchorz fund, the Speijer inheritance fund, and the Goldin-Savad inheritance fund.

## References

1. C.R. Bowers, D.P. Weitekamp, *Phys. Rev. Lett.* **57**(21), 2645–2648 (1986)
2. C.R. Bowers, D.P. Weitekamp, *J. Am. Chem. Soc.* **109**(18), 5541–5542 (1987)
3. T.C. Eischenschmid, R.U. Kirss, P.P. Deutsch, S.I. Hommeltoft, R. Eisenberg, J. Bargon, R.G. Lawler, A.L. Balch, *J. Am. Chem. Soc.* **109**(26), 8089–8091 (1987)
4. J. Natteer, J. Bargon, *Prog. Nucl. Magn. Reson. Spectrosc.* **31**(4), 293–315 (1997)
5. T. Jonischkeit, K. Woelk, *Adv. Synth. Catal.* **346**, 960–969 (2004)
6. S.B. Duckett, C.J. Sleight, *Prog. Nucl. Magn. Reson. Spectrosc.* **34**, 71–92 (1999)
7. K. Golman, O. Axelsson, H. Johannesson, S. Mansson, C. Olofsson, J.S. Petersson, *Magn. Reson. Med.* **46**(1), 1–5 (2001)
8. P. Bhattacharya, K. Harris, A.P. Lin, M. Mansson, V.A. Norton, W.H. Perman, D.P. Weitekamp, B.D. Ross, *Magn. Reson. Mater. Phys. Biol. Med.* **18**(5), 245–256 (2005)
9. P. Bhattacharya, E.Y. Chekmenev, W.H. Perman, K.C. Harris, A.P. Lin, V.A. Norton, C.T. Tan, B.D. Ross, D.P. Weitekamp, *J. Magn. Reson.* **186**(1), 150–155 (2007)
10. H. Johannesson, O. Axelsson, M. Karlsson, *C. R. Physique* **5**(3), 315–324 (2004)
11. K. Golman, R. in't Zandt, M. Thaning, *Proc. Natl. Acad. Sci. USA* **103**(30), 11270–11275 (2006)
12. T.H. Witney, M.I. Kettunen, S.E. Day, D.E. Hu, A.A. Neves, F.A. Gallagher, S.M. Fulton, K.M. Brindle, *Neoplasia* **11**(6), 574–582 (2009)
13. F.A. Gallagher, M.I. Kettunen, D.E. Hu, P.R. Jensen, R. in't Zandt, M. Karlsson, A. Gisselsson, S.K. Nelson, T.H. Witney, S.E. Bohndiek, G. Hansson, T. Peitersen, M.H. Lerche, K.M. Brindle, *Proc. Natl. Acad. Sci. USA* **106**(47), 19801–19806 (2009)
14. S. Aime, W. Dastru, R. Gobetto, A. Viale, *Org. Biomol. Chem.* **3**(21), 3948–3954 (2005)
15. L.S. Bouchard, K.V. Kovtunov, S.R. Burt, M.S. Anwar, I.V. Koptuyug, R.Z. Sagdeev, A. Pines, *Angew. Chem. Int. Ed.* **46**(22), 4064–4068 (2007)
16. J.B. Hovener, E.Y. Chekmenev, K.C. Harris, W.H. Perman, T.T. Tran, B.D. Ross, P. Bhattacharya, *Magn. Reson. Mater. Phys. Biol. Med.* **22**(2), 123–134 (2009)
17. J. Bargon, A. Limbacher, R.R. Rizi, *Int. Soc. Magn. Reson. Med.* **14**, 3111 (2006)
18. M. Matsumoto, J.H. Espenson, *J. Am. Chem. Soc.* **127**(32), 11447–11453 (2005)
19. H.Z. Wang, D.Y.C. Leung, M.K.H. Leung, M. Ni, *Renew. Sust. Energy Rev.* **13**(4), 845–853 (2009)

20. L. Soler, A.M. Candela, J. Macanas, M. Munoz, J. Casado, J. Power Sources **192**(1), 21–26 (2009)
21. T. Jonischkeit, U. Bommerich, J. Stadler, K. Woelk, H.G. Niessen, J. Bargon, J. Chem. Phys. **124**(20), 201109-1–201109-5 (2006)
22. S.B. Duckett, C.L. Newell, R. Eisenberg, J. Am. Chem. Soc. **116**(23), 10548–10556 (1994)
23. X. Wang, L. Andrews, Rev. Sci. Instrum. **75**(9), 3039–3044 (2004)
24. M.G. Pravica, D.P. Weitekamp, Chem. Phys. Lett. **145**, 255–258 (1988)
25. L.T. Kuhn, J. Bargon, Top. Curr. Chem. **276**, 25–68 (2007)
26. M. Goldman, H. Johannesson, O. Axelsson, M. Karlsson, C. R. Chimie **9**(3–4), 357–363 (2006)
27. C.E. Miller, M. Lipsicas, Phys. Rev. **176**(1), 273–279 (1968)
28. K. Golman, A. Oskar, H. Johannesson, European Patent Application EP 1 058 122 A2, 2000
29. D. Canet, C. Aroulanda, P. Mutzenhardt, S. Aime, R. Gobetto, F. Reineri, Concepts Magn. Reson. Part A **28**(5), 321–330 (2006)